

Supporting Information

Two-dimensional Pb square nets from bulk $(RO)_n\text{Pb}$ ($R = \text{rare earth metals}, n = 1,2$)

Xu Chen^{a§}, Jun Deng^{a§}, Shifeng Jin^{a§}, Tianping Ying^{a*}, Ge Fei^b, Huifen Ren^a, Yunfan Yang^{a,c},
Ke Ma^{a,c}, Mingzhang Yang^{a,c}, Junjie Wang^{a,c}, Yanchun Li^d, Xin Chen^b, Xiaobing Liu^b,
Shixuan Du^{a*}, Jian-gang Guo^{a,e*}, Xiaolong Chen^{a,c,e*}

^aBeijing National Laboratory for Condensed Matter Physics, Institute of Physics, Chinese Academy of Sciences, Beijing 100190, China

^bLaboratory of High Pressure Physics and Material Science (HPPMS), School of Physics and Physical Engineering, Qufu Normal University, Qufu 273100, China

^cSchool of Physical Sciences, University of Chinese Academy of Sciences, Beijing 100049, China

^dBeijing Synchrotron Radiation Facility Institute of High Energy Physics, Chinese Academy of Sciences, Beijing 100049, China

^eSongshan Lake Materials Laboratory, Dongguan, Guangdong 523808, China

*ying@iphy.ac.cn, sxdu@iphy.ac.cn, jgguo@iphy.ac.cn, chenx29@iphy.ac.cn

§X.C., J.D. and S.F.J. contributed equally to this paper.

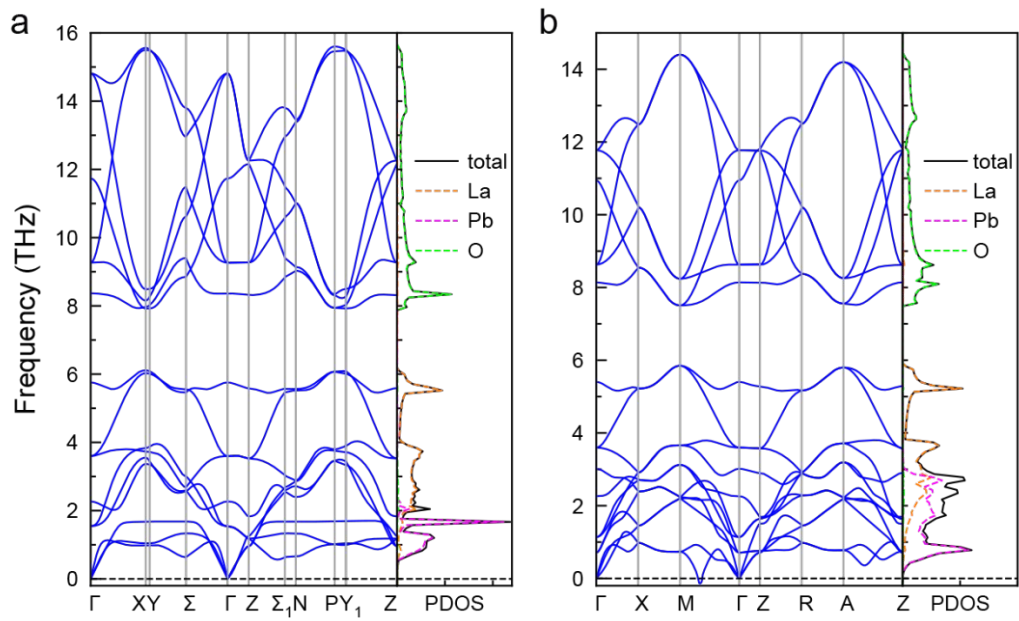


Figure S1. Phonon dispersion for (a) $\text{La}_2\text{O}_2\text{Pb}$ and (b) LaOPb .

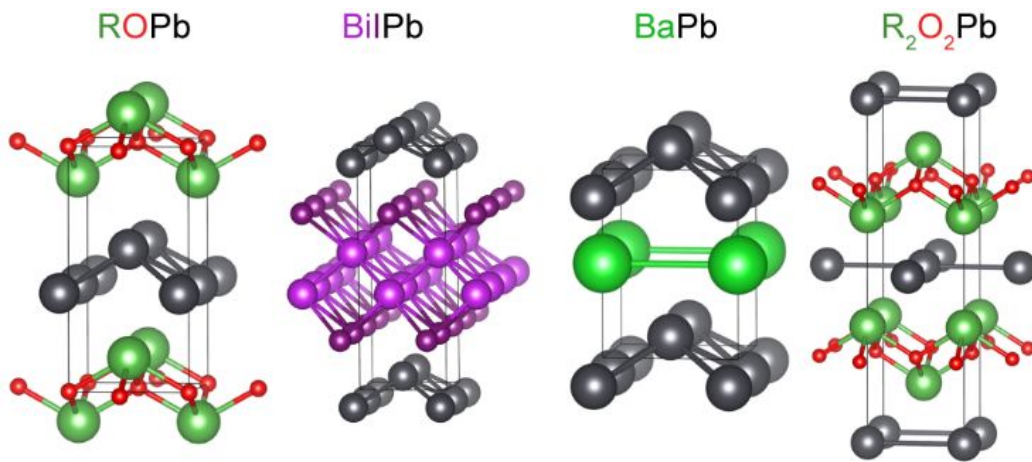


Figure S2. Configurations of the predicted structures in Figure 1(f).

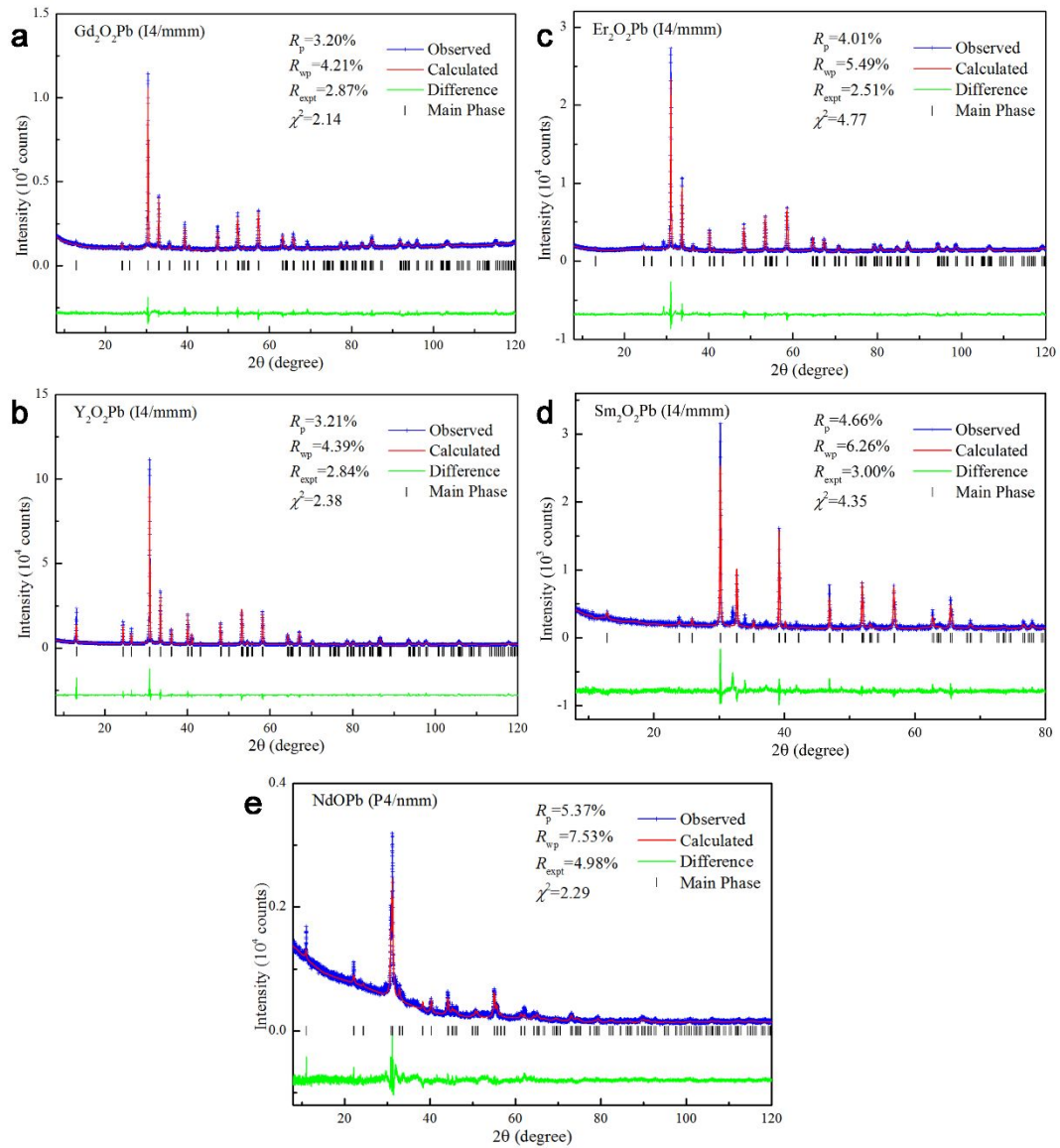


Figure S3. Rietveld refinements of powder X-ray pattern of (a) $\text{Gd}_2\text{O}_2\text{Pb}$, (b) $\text{Y}_2\text{O}_2\text{Pb}$, (c) $\text{Er}_2\text{O}_2\text{Pb}$, (d) $\text{Sm}_2\text{O}_2\text{Pb}$ and (e) NdOPb .

Table S1. Crystallographic parameters of $\text{La}_2\text{O}_2\text{Pb}$, $\text{Sm}_2\text{O}_2\text{Pb}$, $\text{Gd}_2\text{O}_2\text{Pb}$, $\text{Y}_2\text{O}_2\text{Pb}$, $\text{Er}_2\text{O}_2\text{Pb}$, LaOPb and NdOPb .

Compound	$\text{La}_2\text{O}_2\text{Pb}$	$\text{Sm}_2\text{O}_2\text{Pb}$	$\text{Gd}_2\text{O}_2\text{Pb}$	$\text{Y}_2\text{O}_2\text{Pb}$	$\text{Er}_2\text{O}_2\text{Pb}$	LaOPb	NdOPb
Space group	I4/mmm (No. 139)	I4/mmm (No. 139)	I4/mmm (No. 139)	I4/mmm (No. 139)	I4/mmm (No. 139)	P4/nmm (No. 129)	P4/nmm (No. 129)
Z	2	2	2	2	2	2	2
a (Å)	4.0176 (1)	3.8727 (2)	3.8384 (1)	3.7862 (1)	3.7588 (1)	4.1639 (1)	4.0983 (4)
c (Å)	14.2248 (4)	13.7910 (8)	13.7420 (6)	13.4932 (4)	13.4422 (5)	8.2565 (3)	8.0198 (9)
V (Å³)	229.60 (2)	206.84 (3)	202.47 (2)	193.43 (1)	189.91 (1)	143.15 (1)	134.71 (3)
Pb-Pb(Å)	4.0176 (1)	3.8727 (2)	3.8384 (1)	3.7862 (1)	3.7588 (1)	3.718 (3)	3.636 (3)
R_p	4.18%	4.66%	3.20%	3.21%	4.01%	3.45%	5.37%
R_{wp}	5.72%	6.26%	4.21%	4.39%	5.49%	5.06%	7.53%
R_{expt}	3.56%	3.00%	2.87%	2.84%	2.51%	3.62%	4.98%
χ²	2.59	4.35	2.14	2.38	4.77	1.96	2.29
R1	(0, 0, 0.3387 (1))	(0, 0, 0.3366 (2))	(0, 0, 0.3354 (1))	(0, 0, 0.3303 (1))	(0, 0, 0.3357 (3))	(0.25, 0.25, 0.1866 (1))	(0.25, 0.25, 0.1837 (7))
O1	(0, 0.5, 0.25)	(0, 0.5, 0.25)	(0, 0.5, 0.25)	(0, 0.5, 0.25)	(0, 0.5, 0.25)	(0.25, 0.25, 0)	(0.25, 0.25, 0)
Pb1	(0, 0, 0)	(0, 0, 0)	(0, 0, 0)	(0, 0, 0)	(0, 0, 0)	(0.25, 0.25, 0.6375 (1))	(0.25, 0.25, 0.6369 (3))

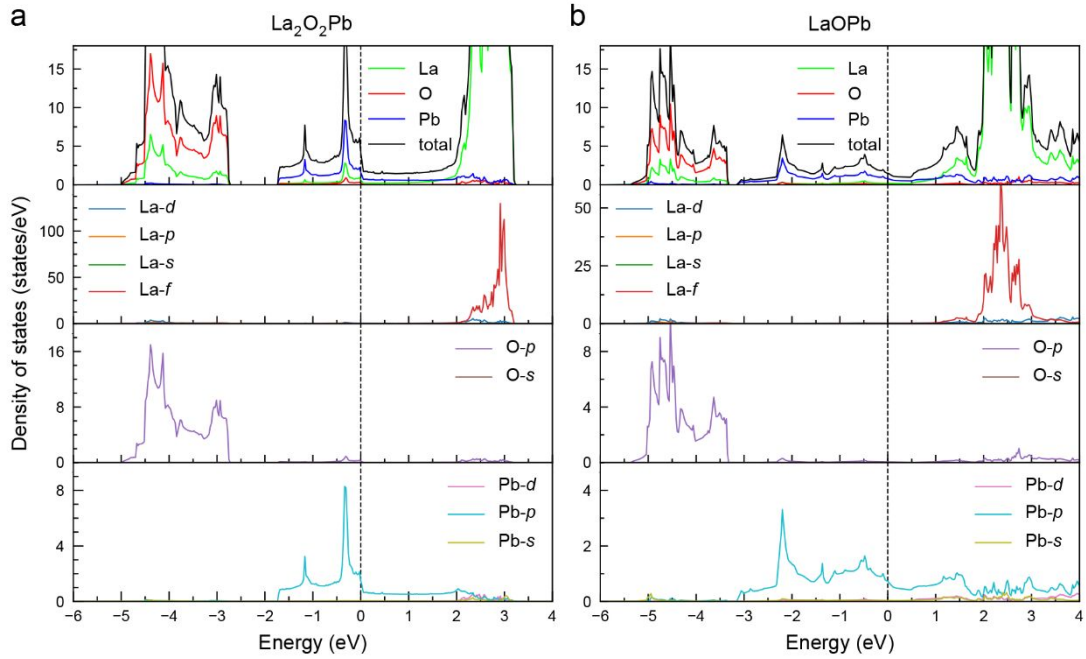


Figure S4. Projected density of states (P-DOS) onto La, O and Pb orbitals of (a) $\text{La}_2\text{O}_2\text{Pb}$ and (b) LaOPb , respectively.

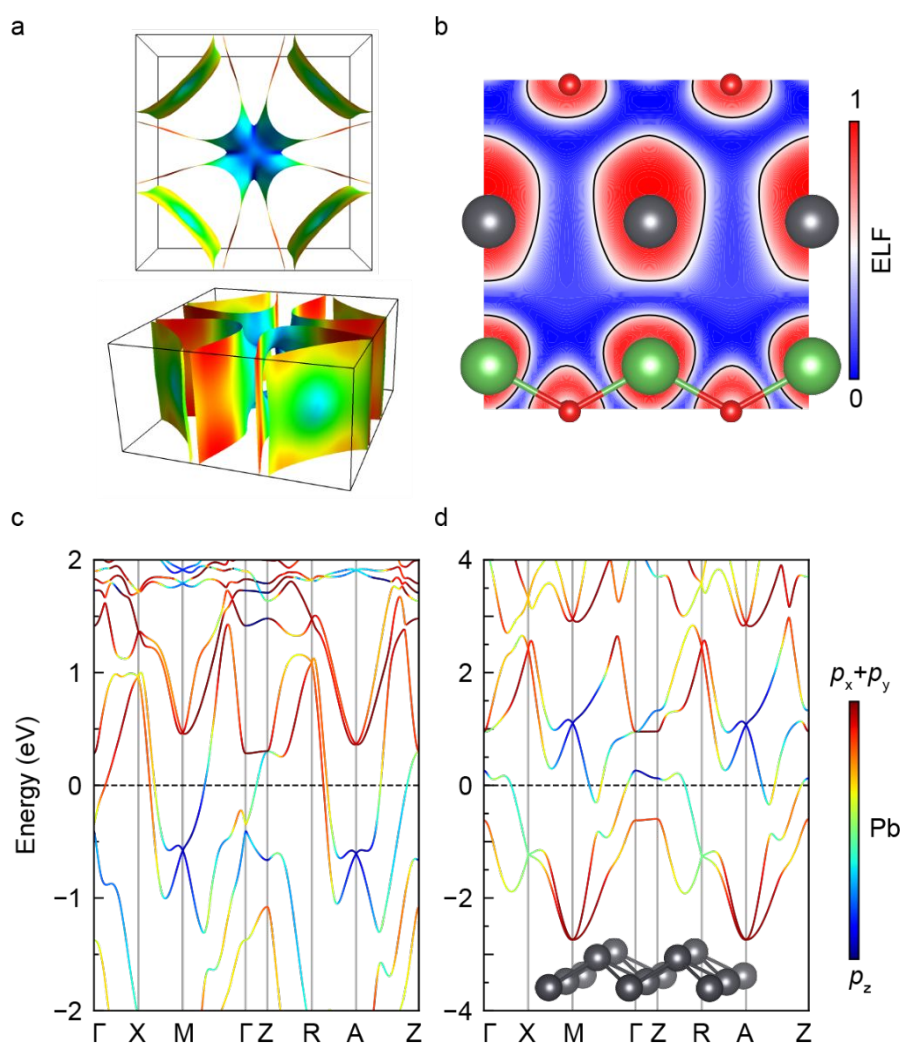


Figure S5. (a) Fermi surface of top (up panel) and side (bottom panel) views, (b) (020)-slice of electron localization function (ELF) crossing La-O-Pb plane. (c) Band structure for LaOPb. (d) Band structure for Pb monolayer, which is obtained by merely removing $[\text{La}_2\text{O}_2]^{2-}$ layers in LaOPb. The color in the band structures labels the states contributed by p_x+p_y and p_z of Pb. The spin-orbit coupling (SOC) is included here.

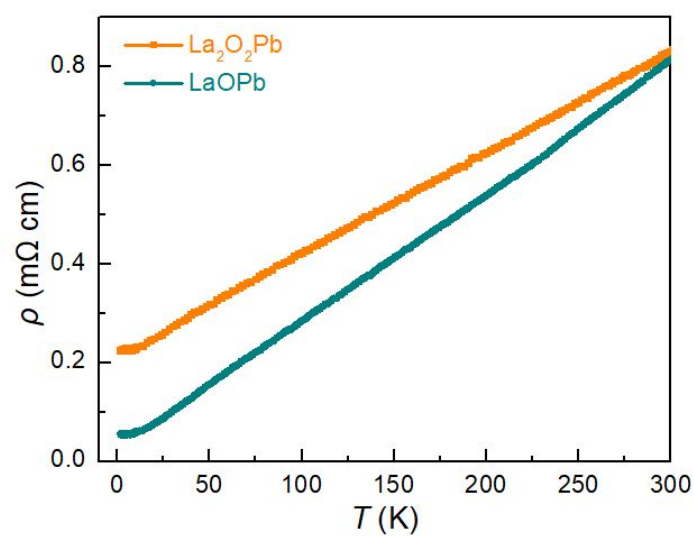


Figure S6. Electrical resistivity (ρ) of LaOPb and La₂O₂Pb as a function of temperature from 2 K to 300 K.

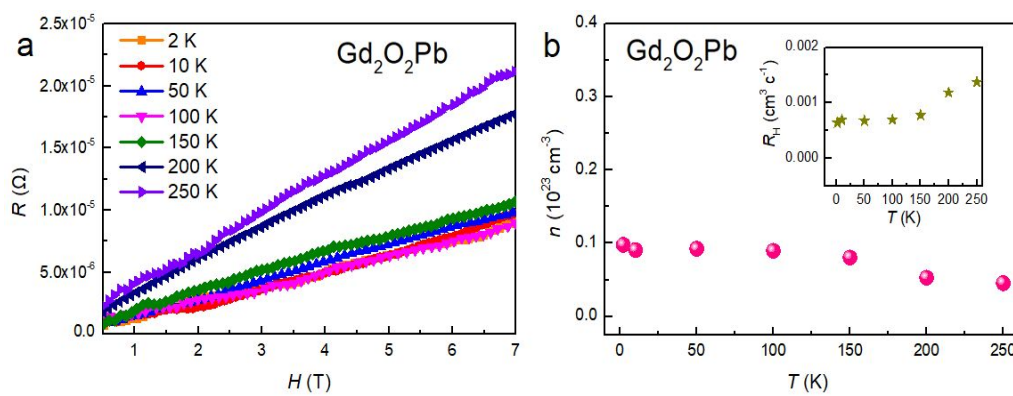


Figure S7. (a) Hall measurements and (b) carrier density of Gd₂O₂Pb.

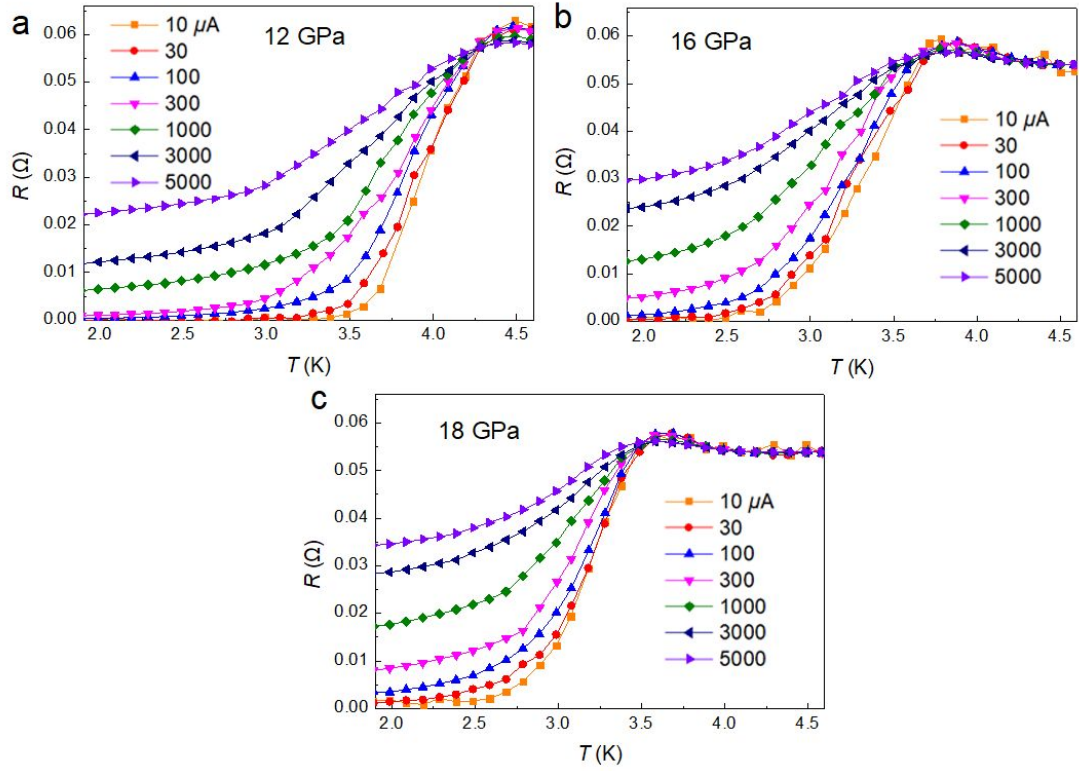


Figure S8. The superconductivity of $\text{Gd}_2\text{O}_2\text{Pb}$ at 12 GPa, 16 GPa and 18 GPa measured at different excitation currents.

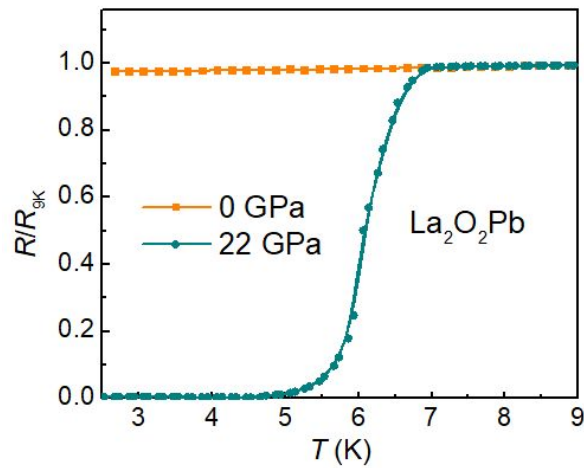


Figure S9. Normalized resistivity of $\text{La}_2\text{O}_2\text{Pb}$ with and without applied external pressure.

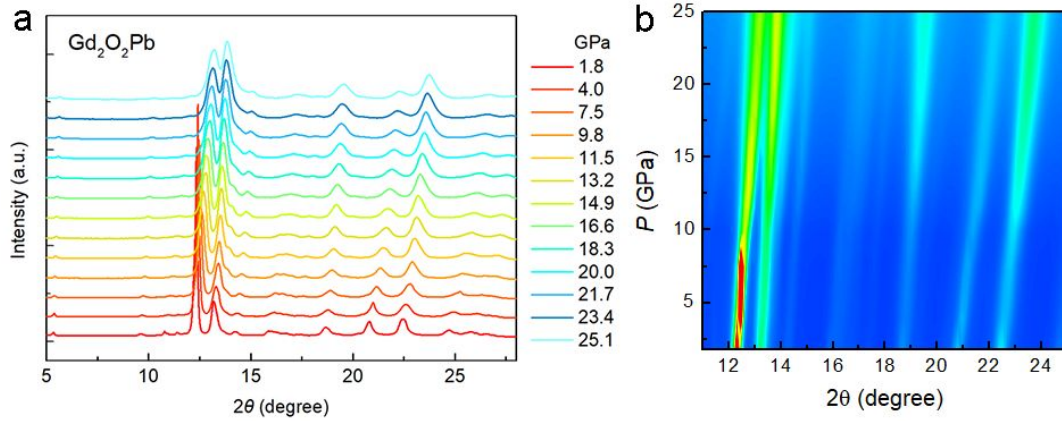


Figure S10. (a) Synchrotron diffraction patterns of $\text{Gd}_2\text{O}_2\text{Pb}$ measured under different pressures from 1.8 to 25 GPa. (b) Color contour of the diffractions with its low angle region shown in Figure 4b.

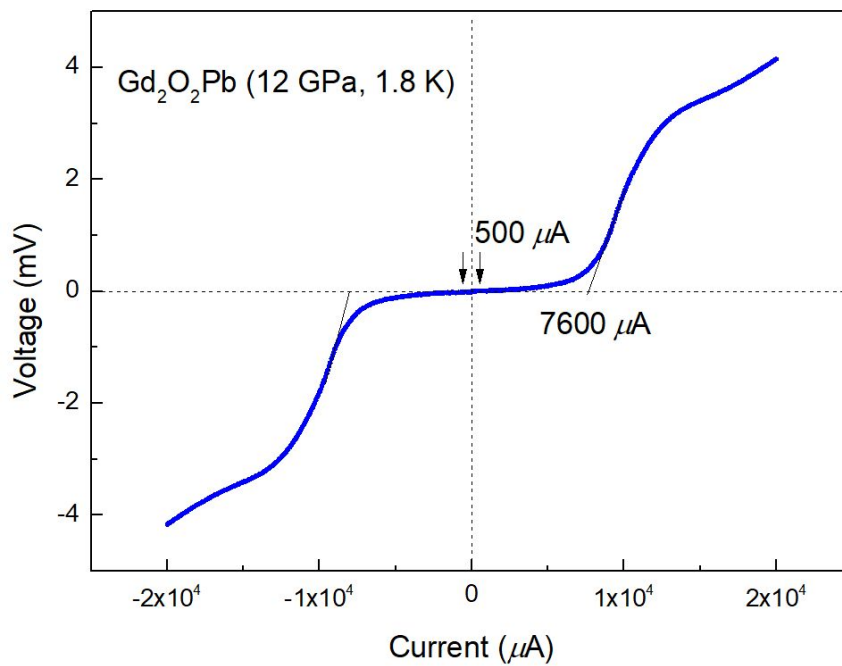


Figure S11. The I - V curves of $\text{Gd}_2\text{O}_2\text{Pb}$ @12 GPa measured at 1.8 K. Arrows in the graph indicate the excitation current required ($500 \mu\text{A}$) to reach zero resistance. The extrapolated solid lines represent the critical current, $J_c = 7600 \mu\text{A}$, of $\text{Gd}_2\text{O}_2\text{Pb}$ at 12 GPa.

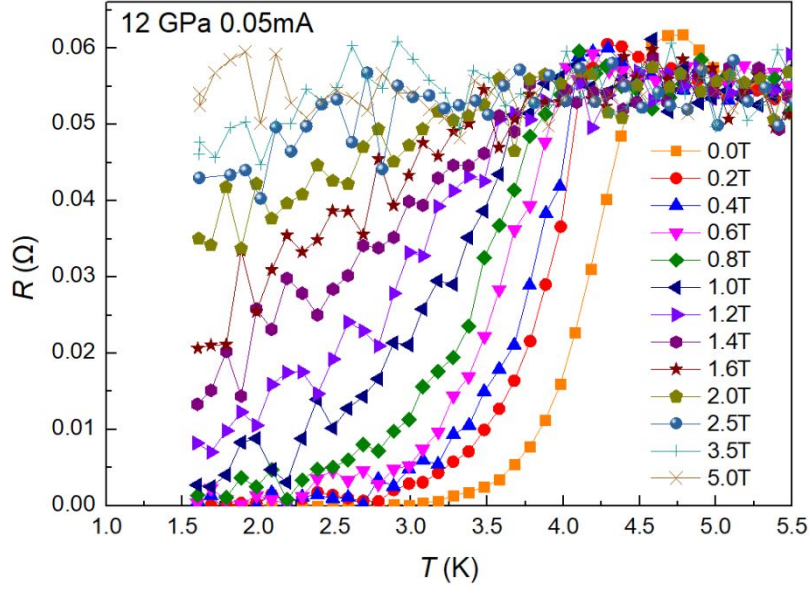


Figure S12. The superconductivity of $\text{Gd}_2\text{O}_2\text{Pb}$ at 12 GPa suppressed by magnetic fields.

Evaluating the thermodynamic of compounds

The thermodynamic stabilities of these structures are evaluated by calculating their phase diagram at 0K. The phase diagrams are constructed as follows. Firstly, the formation enthalpies of them are calculated by:

$$\Delta H = \frac{E(A_xB_yC_z) - xE(A) - yE(B) - zE(C)}{x + y + z} + \Delta c,$$

where $E(A_xB_yC_z)$, $E(A)$, $E(B)$, $E(C)$ are total energy of $A_xB_yC_z$, elements A, B and C under their ground state, respectively. The energy correction term Δc is used to correct the overbonding of gas molecules^{1,2}. Then, the phase diagrams are built by a convex hull analysis of all known compounds in A-B-C phase diagram, which is done by `pymatgen.analysis.phase_diagram` module³. Total energies of known compounds are obtained by Materials Project REST API⁴ except for our predicted ones. In calculating the total energy of $A_xB_yC_z$, an energy cutoff of 520 eV and "potpaw_PBE" type of pseudopotential are used to be consistent with Materials Project.

1. Wang, L.; Maxisch, T.; Ceder, G., Oxidation energies of transition metal oxides within the GGA+U framework. *Phys. Rev. B* **2006**, *73* (19).
2. Jain, A.; Hautier, G.; Ong, S. P.; Moore, C. J.; Fischer, C. C.; Persson, K. A.; Ceder, G., Formation enthalpies by mixing GGA and GGA+U calculations. *Phys. Rev. B* **2011**, *84* (4).
3. Ong, S. P.; Richards, W. D.; Jain, A.; Hautier, G.; Kocher, M.; Cholia, S.; Gunter, D.; Chevrier, V. L.; Persson, K. A.; Ceder, G., Python Materials Genomics (pymatgen): A robust, open-source python library for materials analysis. *Comput. Mater. Sci.* **2013**, *68*, 314-319.
4. Ong, S. P.; Cholia, S.; Jain, A.; Brafman, M.; Gunter, D.; Ceder, G.; Persson, K. A., The Materials Application Programming Interface (API): A simple, flexible and efficient API for materials data based on REpresentational State Transfer (REST) principles. *Comput. Mater. Sci.* **2015**, *97*, 209-215.